THE JOURNAL OF PHYSICAL CHEMISTRY LETTERS
A JOURNAL OF THE AMERICAN CHEMICAL SOCIETY

pubs.acs.org/JPCL Letter

Vibronic Conical Intersection Trajectory Signatures in Wave Packet Coherences

Indranil Ghosh, Qijie Shen, Ping-Jui Eric Wu, and Gregory S. Engel*

Cite This: J. Phys. Chem. Lett. 2024, 15, 12494−12500 Read Online

ACCESS | Metrics & More | Article Recommendations | Supporting Information

ABSTRACT: Conical intersections are ubiquitous in the energy landscape of chemical systems, drive photochemical reactivity, and are extremely challenging to observe spectroscopically. Using two-dimensional electronic spectroscopy, we observe the nonadiabatic dynamics in Wurster's Blue after excitation to the lowest two vibronic excited states. The excited populations relax ballistically through a conical intersection in 55 fs to the electronic ground state potential energy surface as the molecule undergoes an intramolecular electron transfer. While the kinetics are identical on both vibronic energy surfaces, we observe different patterns of coherent oscillations after traversing the conical intersection indicating distinct nonadiabatic relaxation pathways through the conical energetic funnel. These coherences are not created directly by the excitation pulses but are the result of the dynamical trajectories projecting differently on the conical intersection vibrational space. Our spectroscopic data offers a fresh perspective into the complex conical intersection topology and dynamics that emphasizes the critical involvement of the intersection space in dictating the dynamics.

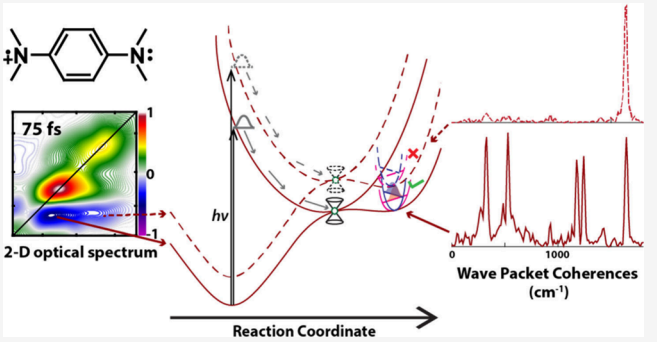

Following an electronic excitation by a photon, energy in the chemical system can relax radiatively or nonradiatively. Radiative relaxation involves emitting a photon, whereas nonradiative relaxation involves dissipation of energy into vibrational modes. Nonradiative relaxation requires vibrational modes to couple to electronic states. This nonadiabatic coupling arises when the energy gap between electronic states is comparable to that of vibrational states. An extreme case of such coupling arises when two electronic surfaces cross at a given nuclear geometry. In other words, the potential energy surfaces create a cone-shaped funnel called a conical intersection.[1−3] Conical intersections may be required by symmetry in symmetric systems, or they can be "accidental," which is both more common and more challenging to predict.[4] This extreme nonadiabatic feature of the electronic structure governs the cis−trans isomerization in critical biological chromophores,[5] influences singlet fission,[6] plays a central role in photochemical reactions,[7] and explains the photostability of chemical systems.[8]

Spectroscopically interrogating conical intersection dynamics in the condensed phase is crucial for testing advanced theoretical models and understanding the complex photophysics near a conical intersection.[4,9] The two vibrational modes that lift the electronic degeneracy linearly in the immediate vicinity of a conical intersection constitute the branching space, while all other modes constitute the intersection space.[3] Advanced spectroscopic and computational studies are starting to demonstrate the effects of the intersection space modes in the ultrafast dynamics near a conical intersection.[10−12] Recently, Subotnik and co-workers showed theoretically that a system with an odd number of electrons undergoes spin separation at the conical intersection due to distinct Berry curvature effects arising from the spin−orbit coupling.[13] These spin effects point toward the importance of fully accounting for both linear and angular momentum conservation in dynamics calculations at the intersection.[14] Here, we use ultrafast electronic spectroscopy on a stable organic radical cation with a conical intersection to measure the time scale of conical intersection traversal with sub-10 fs pulses and observe distinct coherent oscillations by resolving in excitation energy. We correlate these differences to the initial vibronic state.

Wurster's Blue is a stable organic radical cation under standard conditions with perchlorate as the counterion (see Figure 1a). N,N,N′,N′-Tetramethyl-p-phenylenediamine (TMPD) purchased from Enamine was used as the starting material to synthesize Wurster's Blue perchlorate following a one-step oxidation method (see Supporting Information

Received: October 14, 2024
Revised: December 6, 2024
Accepted: December 9, 2024
Published: December 13, 2024

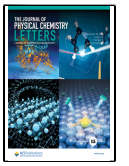

https://doi.org/10.1021/acs.jpclett.4c02979
J. Phys. Chem. Lett. 2024, 15, 12494−12500

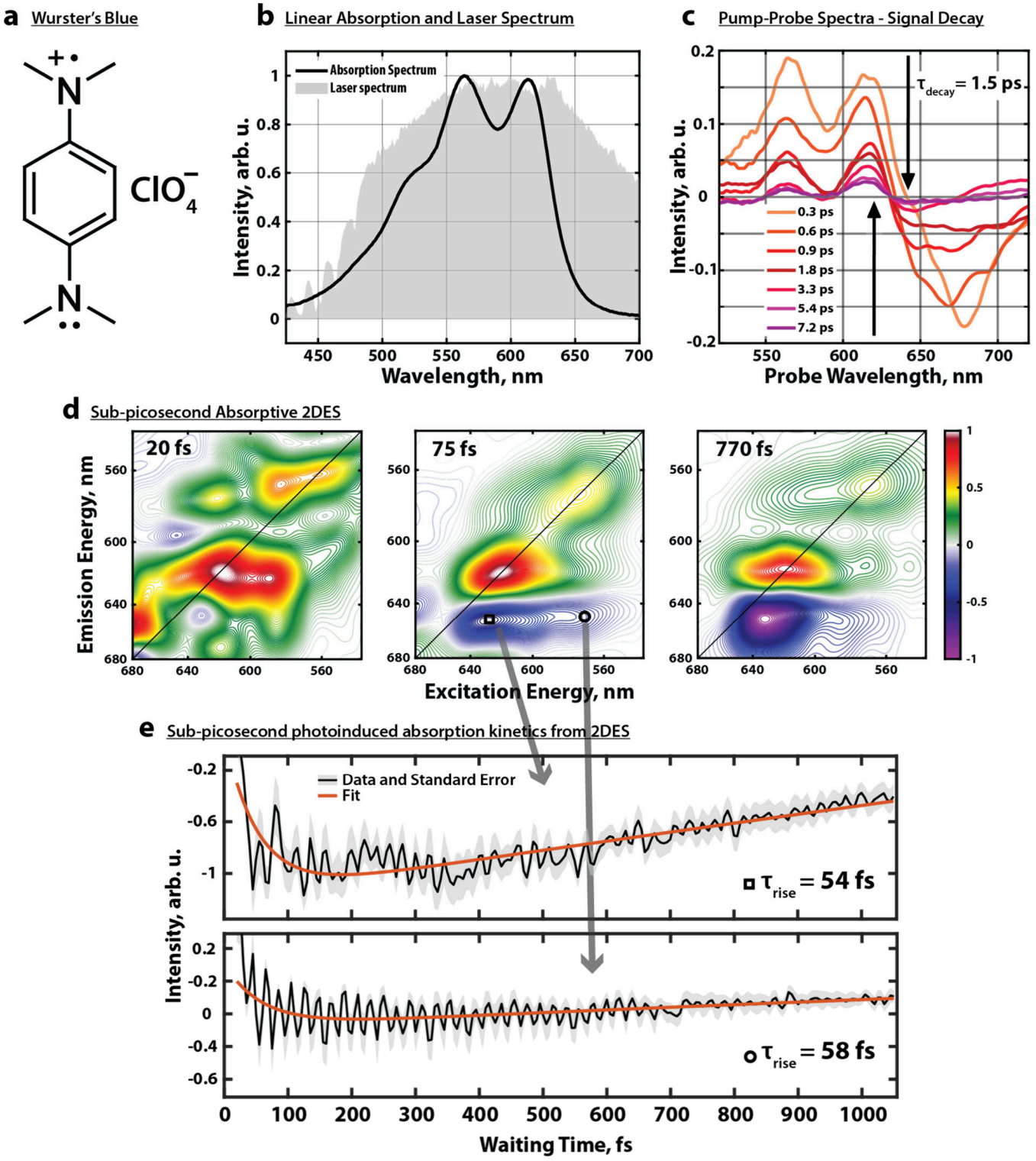

Figure 1. Linear Absorption and Ultrafast Spectroscopy of Wurster's Blue. (a) Chemical structure of Wurster's Blue perchlorate. All experiments were conducted in a MeOH/EtOH 1:1 solvent mixture at room temperature. (b) Linear absorption spectrum of Wurster's Blue and the laser spectrum for all nonlinear spectroscopy experiments. (c) Pump−probe spectra show the decay of transient absorption signal happening in 1.5 ps. (d) Absorptive 2DES correlation maps at three different waiting times (electronic population evolution). The negative photoinduced absorption signature is not seen in 20 fs but appears by 75 fs and persists in the 770 fs frame. (e) Waiting time traces from two locations of the 2DES spectra as denoted in the 75 fs frame in d. Black squares represent electronic population after traversing the conical intersection that was generated by exciting to the $|e_0\rangle$ state (zero quantum in the ring-breathing mode). Black circles represent population after traversing the conical intersection that was generated by exciting to the $|e_1\rangle$ state (one quantum in the ring-breathing mode).

Section 1).[15] Following oxidation, we observe a characteristic intramolecular electron transfer transition.[16,17] This transition couples strongly to the 1641 cm^{-1} benzene ring-breathing mode,[18] giving rise to peaks at 570 and 625 nm in the

https://doi.org/10.1021/acs.jpclett.4c02979
J. Phys. Chem. Lett. 2024, 15, 12494−12500

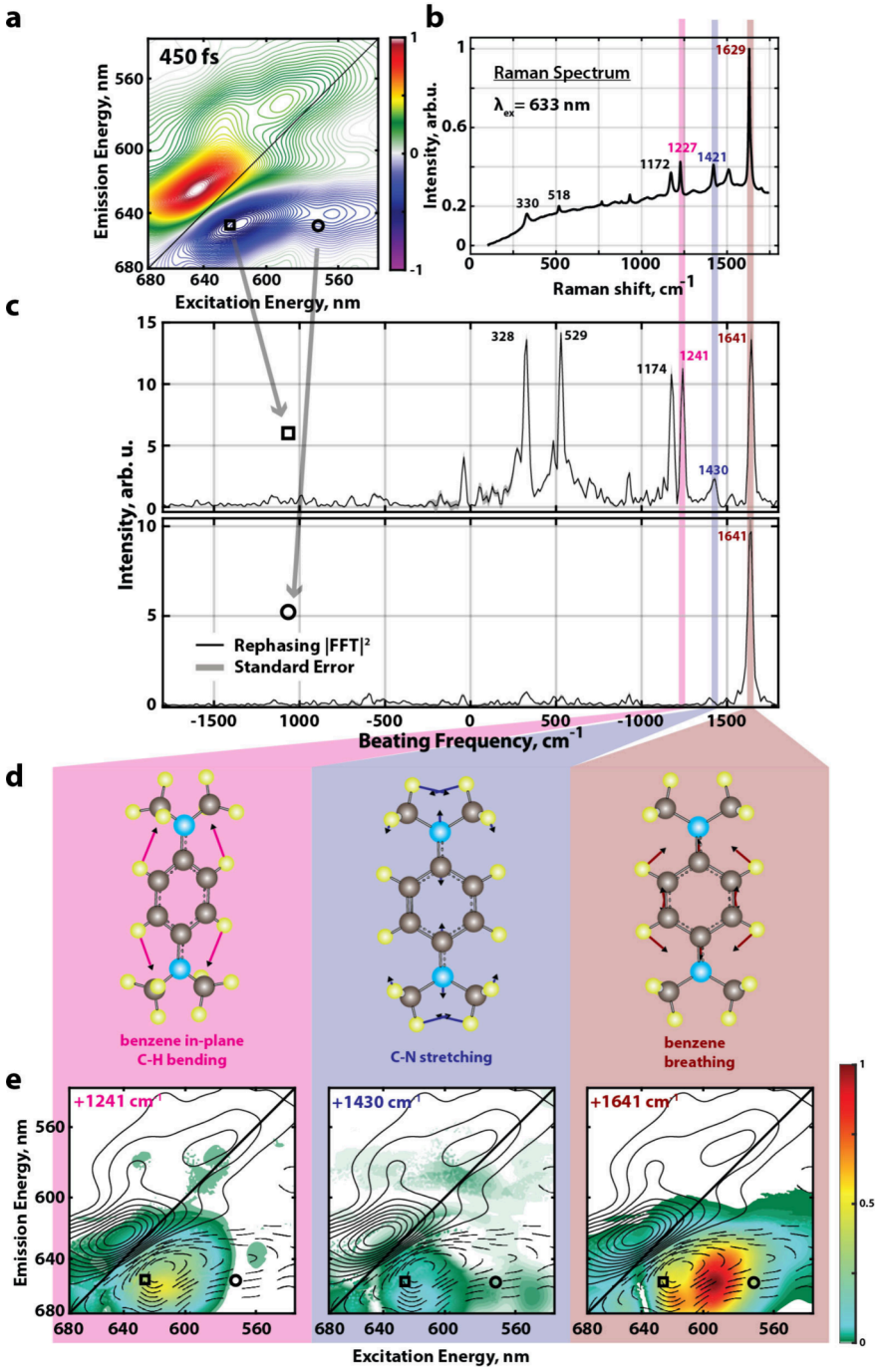

Figure 2. Distinct Vibrational Coherences of the Two PIA Features. (a) Rephasing 2DES spectrum at a waiting time of 450 fs. (b) Raman spectrum corresponds to an excitation at 633 nm. (c) Power spectra of the waiting time signal after subtracting kinetic fits from the rephasing photoinduced absorption 2DES signal at the two excitation energies. (d) Three representative normal modes obtained from the optimized ground state geometry[40] of Wurster's Blue. C_{ring}−N stretching is the tuning mode of the conical intersection branching space. The in-plane C−H bending mode is one of many intersection space modes. The ring-breathing mode is the intersection space mode that couples strongly to the electronic transition, thereby splitting the absorption into two features at 625 nm ($|e_0\rangle$) and 570 nm ($|e_1\rangle$). (e) Beating maps of three specific modes whose motion is depicted in d. Black solid and dashed contours denote positive and negative features of the spectrum shown in a. Colored contours denote the squared amplitude for the specific mode. All three frames are normalized to the maximum intensity of the ring-breathing mode. Only the ring-breathing mode is common to both photoinduced absorption signatures.

absorption spectrum (see Figure 1b). Vauthey and co-workers conducted pump−probe experiments on Wurster's Blue in solution that showed a photoinduced absorption feature appearing by 200 fs.[19] Their fluorescence study indicated a negligible quantum yield at room temperature, implying efficient nonradiative relaxation after photoexcitation. Theoretical calculations supporting these experiments established the presence of a conical intersection connecting the doublet ground and excited electronic states with the C_{ring}−N stretching and the C_{ring}−N torsion modes defining the intersection branching plane.[20]

https://doi.org/10.1021/acs.jpclett.4c02979
J. Phys. Chem. Lett. 2024, 15, 12494−12500

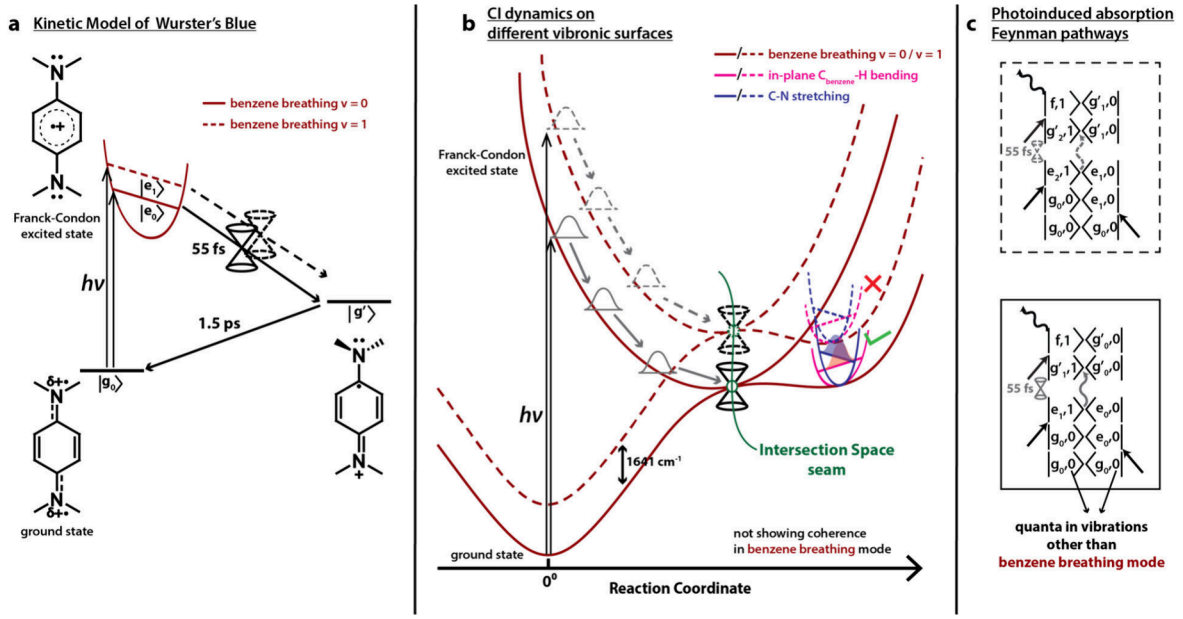

Figure 3. Kinetic Model and Coherent Wave Packet Dynamics. (a) The kinetic model of Wurster's Blue. The vibrational levels in the parabolic potential energy curve correspond to the benzene ring-breathing mode. (b) Vibronic states constructed after coupling to the ring-breathing mode; coherence in this mode is universally present and hence ignored. Different coherences on the two vibronic populations serve as a memory of both their distinct Franck−Condon excitations and conical intersection trajectories. (c) Feynman pathways corresponding to the two photoinduced absorption features indicated by the solid/dashed boxes.

We conduct time-resolved two-dimensional electronic spectroscopy (2DES) experiments on Wurster's Blue at room temperature in 1:1 v/v MeOH/EtOH. Nonlinear spectroscopy techniques with ultrashort pulses have been extensively used in the past few decades to probe nonadiabatic dynamics in the condensed phase.[6,21−25] Details of the apparatus are reported elsewhere.[26] Briefly, 2DES can track excited electronic state populations in time while resolving both the excitation and emission energies. Third-order nonlinear signals are broadly classified into ground state bleach (GSB), stimulated emission (SE), and photoinduced absorption (PIA). 2DES experiments of Wurster's Blue show two photoinduced absorption (PIA) features corresponding to excitation in the two excited vibronic states, $|e_0\rangle$ and $|e_1\rangle$, where the suffix indicates the number of quanta in the ring-breathing mode. Using sub-10 fs pulses (see Supporting Information Section 2), we obtain a 55 fs time constant for the growth of both PIA features (see Figure 1e). This time scale is much shorter than 200 fs reported previously,[20] indicating a ballistic wave packet traversal through the conical intersection. Ground state bleach recovery and the disappearance of the PIA signal occur with a time constant of 1.5 ps (see Figure 1c and Figure S5), which are consistent with Vauthey and co-workers' findings[20] and make Wurster's Blue a promising candidate for efficient molecular photoswitches.[27,28]

We observe a clear coherent oscillation in waiting time corresponding to the vibrational coherence of the 1641 cm^{-1} ring-breathing mode (see Figure 1e). This is the same mode that couples strongly to the electronic transition, giving rise to a vibronic progression in the absorption spectrum (see Figure S3). To understand the microscopic origin of this oscillation, we separate our absorptive spectrum into rephasing and nonrephasing portions and focus our analysis on the rephasing spectra (see Figure 2a), which contain signatures that can be unambiguously assigned to the excited state. In Figure 2, we see that the additional modes appear at the location of the PIA features; these modes show positive frequencies. To understand the origin of these signals, we analyze the Feynman pathways that can give rise to positive frequencies in this spectral region (see Figure 3c).[29] The modes we observe have energy gaps far larger than k_BT at room temperature, and we can, therefore, limit our analysis to those pathways that start in the vibrational ground state. The beating signals at the PIA spectral position can only have a positive frequency, i.e., $e^{+i\omega t}$, on the electronic population that traversed the conical intersection. In contrast, a ground state bleach feature would have a negative frequency, i.e., $e^{-i\omega t}$, though such a signal would not be likely to appear at this spectral location (see Figure 2).[30] Similar analysis has been exploited previously for assigning coherences on the ground or excited electronic states.[31] For the PIA features, the only rephasing Feynman pathways yielding oscillations with positive frequencies are the ones that start on the excited electronic energy surface and traverse through the conical intersection on to the ground electronic potential energy surface (see Figure 3c).

The coherence involving the 1641 cm^{-1} ring-breathing mode is similarly prominent on both vibronic populations after traversal through the conical intersection (see Figure 2c, 2e). Several modes with relatively low activity in the Raman spectrum are as bright as the ring-breathing mode for the population originating from $|e_0\rangle$, while at the same time, all of them are suppressed in the population originating from $|e_1\rangle$, as seen in the beating power spectra corresponding to the two PIA features (see Figure 2). The mode at ∼1430 cm^{-1} corresponds to C_{ring}−N stretching and is the tuning mode of the conical intersection branching space. We see this mode appreciably active in the population launched on $|e_0\rangle$ and in the Raman spectrum, while it is suppressed on that from $|e_1\rangle$. Wurster's Blue belongs to the D_{2h} point group at equilibrium and at the Franck−Condon excited state. The mode at 529 cm^{-1} that corresponds to the C_{ring}−N out-of-plane rocking motion has minimal activity in the resonant Raman spectrum

https://doi.org/10.1021/acs.jpclett.4c02979
J. Phys. Chem. Lett. 2024, 15, 12494−12500

(see Figure 2b) as well as low Franck−Condon activity in the excited state (see Figures S7 and S8) and is Raman inactive under D_{2h} symmetry. However, it is pronounced only for the $|e_0\rangle$ initialized population (see Figure 2c and Figure S10). Because the C_{ring}−N torsion lowers the symmetry in the molecule, a coherence launched along the 529 cm^{-1} mode while traversing the conical intersection may be unsurprising, but its suppression in the population signature following excitation to $|e_1\rangle$ is noteworthy. Rephasing power spectra for all the positive 2DES spectral features and their corresponding Feynman pathways are shown in Figures S7 and S8 respectively. The spectral signatures on the power spectra corresponding to excited state pathways show similar Franck−Condon prefactors for the $|e_0\rangle$ and $|e_1\rangle$ vibronic states. This contrasts with the distinct coherent oscillations of the two populations following traversal of the conical intersection. This observation proves that the electronic populations on the two vibronic surfaces traverse the intersection space differently and therefore represent unique trajectories through the conical intersection. These wave packet coherences contain information on the projection of the vibronic wave packets on to the conical intersection seam. We considered other alternative hypotheses, such as how incorporating Duschinsky rotation effects can give rise to a new set of Franck−Condon overlap integrals between the $|e_0\rangle$ and $|e_1\rangle$ vibronic surfaces,[32] but the largely similar Franck−Condon activities on the two surfaces indicate otherwise. Interference between multiple vibronic coherences may also result in cancellation of coherent signals giving rise to the power spectrum for the population launched from the $|e_1\rangle$ Franck−Condon point.[33]

The PIA signal corresponding to the $|e_0\rangle$ launched population is twice as intense as that for $|e_1\rangle$ suggesting that the nonequilibrium population yield after traversing the conical intersection may differ. However, signal intensity alone cannot definitively indicate the quantum yield arising from different vibronic excited states. Besides quantum yield, the PIA signal intensity also depends on the transition dipole moment between said nonequilibrium state and the higher-lying excited electronic state. The distinct vibrational coherences persisting in the two populations could also modify the net transition-dipole strength due to varied contributions from different modes with different Franck−Condon factors. Similar traversal kinetics with elusive transition-dipole parameters make it difficult to extract quantum yield differences after traversing the conical intersection on the two vibronic surfaces, as has been seen before.[34] We could not definitively assign the photoinduced absorption feature to a photoproduct or a hot ground state population. An isosbestic point between the PIA and the GSB features (see Figure 1c) indicates the presence of a population in a separate quantum state, although we were unable to computationally find a metastable photoproduct state. Previous studies by the Vauthey group have assigned the PIA feature to a hot ground state.[19,20,35] We have elaborated on this discussion in Supporting Information Section 3. Wave packet dynamics simulations can help uncover the complete photophysical mechanism and would require incorporating multiple intersection space modes apart from the two branching space modes. Constructing diabatic surfaces is often a requirement for such tedious computations and becomes challenging for a multimodal conical intersection scenario.[36] A relatively small system such as Wurster's Blue can serve as a testing bed for approaches for modeling extreme nonadiabatic photophysics.[36−38] Lastly, this system having an odd number of electrons may serve as a model to interrogate the influence of electronic spin and the Berry curvature on dynamics near a conical intersection, though we were not able to identify a signature of this effect.[13,14,39]

Two-dimensional electronic spectroscopy on Wurster's Blue enabled us to observe vibronic excited-state-dependent coherences after traversing a conical intersection by exploiting the excitation energy resolution. We unambiguously determine the conical intersection traversal time scale to be 55 fs, which is much faster than previously known.[19,20] This time scale is the same for both populations originating from the vibration-coupled first electronic excited state. Despite having similar kinetics that usually serve as a marker for nonadiabaticity near a conical intersection, we see stark differences in vibrational coherences in their photoinduced absorption signals. The coherences (or suppression thereof) seen in the populations after traversing the conical intersection are not created by the excitation pulses, which means that they are dynamically projected onto different vibrational modes as they traverse the conical intersection seam. Investigating the role of the intersection space, incorporating the conservation of linear and angular momentum, and the interference between vibronic coherences may contribute to unearthing the experimental observations in this paper.[10−14,33,36] Further investigation of the intersection space, incorporating the conservation of linear and angular momentum, and the interference between vibronic coherences may contribute to unearthing the photophysical mechanism of Wurster's Blue's ultrafast intramolecular electron transfer.

■ ASSOCIATED CONTENT

Supporting Information

The Supporting Information is available free of charge at https://pubs.acs.org/doi/10.1021/acs.jpclett.4c02979.

Wurster's Blue synthesis, pulse characterization, additional spectroscopic data and discussion, computational details (PDF)

■ AUTHOR INFORMATION

Corresponding Author

Gregory S. Engel − *Department of Chemistry, The University of Chicago, Chicago, Illinois 60637, United States; The Institute for Biophysical Dynamics, James Franck Institute, and Pritzker School of Molecular Engineering, The University of Chicago, Chicago, Illinois 60637, United States;* orcid.org/0000-0002-6740-5243; Email: gsengel@uchicago.edu

Authors

Indranil Ghosh − *Department of Chemistry, The University of Chicago, Chicago, Illinois 60637, United States; The Institute for Biophysical Dynamics, James Franck Institute, and Pritzker School of Molecular Engineering, The University of Chicago, Chicago, Illinois 60637, United States;* orcid.org/0000-0003-1789-8825

Qijie Shen − *Department of Chemistry, The University of Chicago, Chicago, Illinois 60637, United States; The Institute for Biophysical Dynamics, James Franck Institute, and Pritzker School of Molecular Engineering, The University of Chicago, Chicago, Illinois 60637, United States;* orcid.org/0000-0003-4660-0960

Ping-Jui Eric Wu − *Department of Chemistry, The University of Chicago, Chicago, Illinois 60637, United States; The Institute for Biophysical Dynamics, James Franck Institute, and Pritzker School of Molecular Engineering, The University of Chicago, Chicago, Illinois 60637, United States*

Complete contact information is available at: https://pubs.acs.org/10.1021/acs.jpclett.4c02979

Author Contributions

I.G. and G.S.E. conceived the research. I.G. performed synthesis of Wurster's Blue. I.G. performed nonlinear spectroscopy experiments. I.G. performed analysis of nonlinear spectroscopy data. Q.S. performed computational chemistry calculations. I.G., Q.S., and P.-J.E.W. performed data modeling. I.G. and G.S.E. wrote the paper. All authors provided feedback on writing.

Notes

The authors declare no competing financial interest.

■ ACKNOWLEDGMENTS

The authors thank Dr. Karen M. Watters for scientific editing. P.-J.E.W. acknowledges the Department of Chemistry at the University of Chicago for the Eugene Olshansky Memorial Fellowship for funding. This work was primarily funded by the Department of Energy through Award No. DE-SC0020131 and benefitted from the financial support provided by the National Science Foundation through QuBBE QLCI (NSF OMA-2121044) and Grant No. CHE-1900359. The authors acknowledge the Research Computing Center at the University of Chicago. This work made use of the shared facilities at the University of Chicago Materials Research Science and Engineering Center, supported by the National Science Foundation under award number DMR-2011854.

■ REFERENCES

(1) Domcke, W.; Yarkony, D.; Köppel, H. *Conical Intersections: Electronic Structure, Dynamics & Spectroscopy*; World Scientific, 2004.
(2) Boeije, Y.; Olivucci, M. From a One-Mode to a Multi-Mode Understanding of Conical Intersection Mediated Ultrafast Organic Photochemical Reactions. *Chem. Soc. Rev.* **2023**, *52* (8), 2643−2687.
(3) Malhado, J. P.; Bearpark, M. J.; Hynes, J. T. Non-Adiabatic Dynamics Close to Conical Intersections and the Surface Hopping Perspective. *Front. Chem.* **2014**, *2* (97), 1−21.
(4) Yarkony, D. R. Diabolical Conical Intersections. *Rev. Mod. Phys.* **1996**, *68* (4), 985−1013.
(5) Polli, D.; Altoè, P.; Weingart, O.; Spillane, K. M.; Manzoni, C.; Brida, D.; Tomasello, G.; Orlandi, G.; Kukura, P.; Mathies, R. A.; Garavelli, M.; Cerullo, G. Conical Intersection Dynamics of the Primary Photoisomerization Event in Vision. *Nature* **2010**, *467* (7314), 440−443.
(6) Musser, A. J.; Liebel, M.; Schnedermann, C.; Wende, T.; Kehoe, T. B.; Rao, A.; Kukura, P. Evidence for Conical Intersection Dynamics Mediating Ultrafast Singlet Exciton Fission. *Nature Phys.* **2015**, *11* (4), 352−357.
(7) Karashima, S.; Humeniuk, A.; Uenishi, R.; Horio, T.; Kanno, M.; Ohta, T.; Nishitani, J.; Mitrić, R.; Suzuki, T. Ultrafast Ring-Opening Reaction of 1,3-Cyclohexadiene: Identification of Nonadiabatic Pathway via Doubly Excited State. *J. Am. Chem. Soc.* **2021**, *143* (21), 8034−8045.
(8) Toldo, J. M.; do Casal, M. T.; Barbatti, M. Mechanistic Aspects of the Photophysics of UVA Filters Based on Meldrum Derivatives. *J. Phys. Chem. A* **2021**, *125* (25), 5499−5508.
(9) Keefer, D.; Schnappinger, T.; De Vivie-Riedle, R.; Mukamel, S. Visualizing Conical Intersection Passages via Vibronic Coherence Maps Generated by Stimulated Ultrafast X-Ray Raman Signals. *Proc. Natl. Acad. Sci. U.S.A.* **2020**, *117* (39), 24069−24075.
(10) Yang, X.; Manathunga, M.; Gozem, S.; Léonard, J.; Andruniów, T.; Olivucci, M. Quantum−Classical Simulations of Rhodopsin Reveal Excited-State Population Splitting and Its Effects on Quantum Efficiency. *Nat. Chem.* **2022**, *14* (4), 441−449.
(11) List, N. H.; Jones, C. M.; Martínez, T. J. Internal Conversion of the Anionic GFP Chromophore: In and out of the I-Twisted S_1/S_0 Conical Intersection Seam. *Chem. Sci.* **2022**, *13* (2), 373−385.
(12) Ridente, E.; Hait, D.; Haugen, E. A.; Ross, A. D.; Neumark, D. M.; Head-Gordon, M.; Leone, S. R. Femtosecond Symmetry Breaking and Coherent Relaxation of Methane Cations via X-Ray Spectroscopy. *Science* **2023**, *380* (6646), 713−717.
(13) Wu, Y.; Subotnik, J. E. Electronic Spin Separation Induced by Nuclear Motion near Conical Intersections. *Nat. Commun.* **2021**, *12* (1), 700.
(14) Wu, Y.; Rawlinson, J.; Littlejohn, R. G.; Subotnik, J. E. Linear and Angular Momentum Conservation in Surface Hopping Methods. *J. Chem. Phys.* **2024**, *160* (2), No. 024119.
(15) Michaelis, L.; Granick, S. The Polymerization of the Free Radicals of the Wurster Dye Type: The Dimeric Resonance Bond. *J. Am. Chem. Soc.* **1943**, *65* (9), 1747−1755.
(16) Albrecht, A. C.; Simpson, W. T. Spectroscopic Study of Wurster's Blue and Tetramethyl-p-Phenylenediamine with Assignments of Electronic Transitions ^{1}. *J. Am. Chem. Soc.* **1955**, *77* (17), 4454−4461.
(17) Mayer, M. G.; McCallum, K. J. Calculation of the Absorption Spectrum of Wurster's Salts. *Rev. Mod. Phys.* **1942**, *14* (2−3), 248−257.
(18) Kubinyi, M.; Varsányi, G.; Grofcsik, A. Vibrational Study of N,N,N′,N′-Tetramethyl-p-Phenylenediamine and Its Radical Cation. *Spectrochimica Acta Part A: Molecular Spectroscopy* **1980**, *36* (3), 265−272.
(19) Grilj, J.; Buchgraber, P.; Vauthey, E. Excited-State Dynamics of Wurster's Salts. *J. Phys. Chem. A* **2012**, *116* (28), 7516−7522.
(20) Grilj, J.; Laricheva, E. N.; Olivucci, M.; Vauthey, E. Fluorescence of Radical Ions in Liquid Solution: Wurster's Blue as a Case Study. *Angew. Chem., Int. Ed.* **2011**, *50* (19), 4496−4498.
(21) Hart, S. M.; Banal, J. L.; Bathe, M.; Schlau-Cohen, G. S. Identification of Nonradiative Decay Pathways in Cy3. *J. Phys. Chem. Lett.* **2020**, *11* (13), 5000−5007.
(22) Dean, J. C.; Rather, S.; Oblinsky, D. G.; Cassette, E.; Jumper, C. C.; Scholes, G. D. Broadband Transient Absorption and Two-Dimensional Electronic Spectroscopy of Methylene Blue. *J. Phys. Chem. A* **2015**, *119* (34), 9098−9108.
(23) Huang-Fu, Z.-C.; Tkachenko, N. V.; Qian, Y.; Zhang, T.; Brown, J. B.; Harutyunyan, A.; Chen, G.; Rao, Y. Conical Intersections at Interfaces Revealed by Phase-Cycling Interface-Specific Two-Dimensional Electronic Spectroscopy (i2D-ES). *J. Am. Chem. Soc.* **2024**, *146* (30), 20996−21007.
(24) Schnedermann, C.; Yang, X.; Liebel, M.; Spillane, K. M.; Lugtenburg, J.; Fernández, I.; Valentini, A.; Schapiro, I.; Olivucci, M.; Kukura, P.; Mathies, R. A. Evidence for a Vibrational Phase-Dependent Isotope Effect on the Photochemistry of Vision. *Nature Chem.* **2018**, *10* (4), 449−455.
(25) Kitney-Hayes, K. A.; Ferro, A. A.; Tiwari, V.; Jonas, D. M. Two-Dimensional Fourier Transform Electronic Spectroscopy at a Conical Intersection. *J. Chem. Phys.* **2014**, *140* (12), No. 124312.
(26) Zheng, H.; Caram, J. R.; Dahlberg, P. D.; Rolczynski, B. S.; Viswanathan, S.; Dolzhnikov, D. S.; Khadivi, A.; Talapin, D. V.; Engel, G. S. Dispersion-Free Continuum Two-Dimensional Electronic Spectrometer. *Appl. Opt.* **2014**, *53* (9), 1909.
(27) Volarić, J.; Szymanski, W.; Simeth, N. A.; Feringa, B. L. Molecular Photoswitches in Aqueous Environments. *Chem. Soc. Rev.* **2021**, *50* (22), 12377−12449.
(28) Filatov, M.; Paolino, M.; Pierron, R.; Cappelli, A.; Giorgi, G.; Léonard, J.; Huix-Rotllant, M.; Ferré, N.; Yang, X.; Kaliakin, D.; Blanco-González, A.; Olivucci, M. Towards the Engineering of a

Photon-Only Two-Stroke Rotary Molecular Motor. *Nat. Commun.* **2022**, *13* (1), 6433.
(29) Hamm, P.; Zanni, M. *Concepts and Methods of 2D Infrared Spectroscopy*; Cambridge University Press: Cambridge, 2011. DOI: 10.1017/CBO9780511675935.
(30) Butkus, V.; Zigmantas, D.; Valkunas, L.; Abramavicius, D. Vibrational vs. Electronic Coherences in 2D Spectrum of Molecular Systems. *Chem. Phys. Lett.* **2012**, *545*, 40−43.
(31) Higgins, J. S.; Allodi, M. A.; Lloyd, L. T.; Otto, J. P.; Sohail, S. H.; Saer, R. G.; Wood, R. E.; Massey, S. C.; Ting, P.-C.; Blankenship, R. E.; Engel, G. S. Redox Conditions Correlated with Vibronic Coupling Modulate Quantum Beats in Photosynthetic Pigment−Protein Complexes. *Proc. Natl. Acad. Sci. U.S.A.* **2021**, *118* (49), No. e2112817118.
(32) Arpin, P. C.; Popa, M.; Turner, D. B. Signatures of Duschinsky Rotation in Femtosecond Coherence Spectra. *AppliedMath* **2022**, *2* (4), 675−686.
(33) Farfan, C. A.; Turner, D. B. Interference among Multiple Vibronic Modes in Two-Dimensional Electronic Spectroscopy. *Mathematics* **2020**, *8* (2), 157.
(34) Zgrablić, G.; Novello, A. M.; Parmigiani, F. Population Branching in the Conical Intersection of the Retinal Chromophore Revealed by Multipulse Ultrafast Optical Spectroscopy. *J. Am. Chem. Soc.* **2012**, *134* (2), 955−961.
(35) Kumpulainen, T.; Lang, B.; Rosspeintner, A.; Vauthey, E. Ultrafast Elementary Photochemical Processes of Organic Molecules in Liquid Solution. *Chem. Rev.* **2017**, *117* (16), 10826−10939.
(36) Subotnik, J. E.; Alguire, E. C.; Ou, Q.; Landry, B. R.; Fatehi, S. The Requisite Electronic Structure Theory To Describe Photoexcited Nonadiabatic Dynamics: Nonadiabatic Derivative Couplings and Diabatic Electronic Couplings. *Acc. Chem. Res.* **2015**, *48* (5), 1340−1350.
(37) Hennefarth, M.; Hermes, M. R.; Truhlar, D. G.; Gagliardi, L. Analytic Nuclear Gradients for Complete Active Space Linearized Pair-Density Functional Theory. *J. Chem. Theory Comput.* **2024**, *20* (9), 3637.
(38) Wong, M. T.; Cheng, Y.-C. A Quantum Langevin Equation Approach for Two-Dimensional Electronic Spectra of Coupled Vibrational and Electronic Dynamics. *J. Chem. Phys.* **2021**, *154* (15), No. 154107.
(39) Chandran, S. S.; Wu, Y.; Teh, H.-H.; Waldeck, D. H.; Subotnik, J. E. Electron Transfer and Spin−Orbit Coupling: Can Nuclear Motion Lead to Spin Selective Rates? *J. Chem. Phys.* **2022**, *156* (17), No. 174113.
(40) Frisch, M. J.; Trucks, G. W.; Schlegel, H. B.; Scuseria, G. E.; Robb, M. A.; Cheeseman, J. R.; Scalmani, G.; Barone, V.; Petersson, G. A.; Nakatsuji, H.; Li, X.; Caricato, M.; Marenich, A. V.; Blolino, J.; Janesko, B. G.; Gomperts, R.; Mennucci, B.; Hratchian, H. P.; Ortiz, J. V.; Izmaylov, A. F.; Sonnenberg, J. L.; Williams-Young, D.; Ding, F.; Lipparini, F.; Egidi, F.; Goings, J.; Peng, B.; Petrone, A.; Henderson, T.; Ranasinghe, D.; Zakrzewski, V. G.; Gao, J.; Rega, N.; Zheng, G.; Liang, W.; Hada, M.; Ehara, M.; Toyota, K.; Fukuda, R.; Hasegawa, J.; Ishida, M.; Nakajima, T.; Honda, Y.; Kitao, O.; Nakai, H.; Vreven, T.; Throssell, K.; Montgomery, J. A., Jr.; Peralta, J. E.; Oligaro, F.; Bearpark, M. J.; Heyd, J. J; Brothers, E. N.; Kudin, K. N.; Staroverov, V. N.; Keith, T. A.; Kobayashi, R.; Normand, J.; Ragavachari, K.; Rendell, A. P.; Burant, J. C.; Iyengar, S. S.; Tomasi, J.; Cossi, M.; Millam, J. M.; Klene, M.; Adamo, C.; Cammi, R.; Ochterski, J. W.; Martin, R. L.; Morokuma, K.; Farkas, O.; Foresman, J. B.; Fox, D. J. *Gaussian 16*, revision A.03; Gaussian, Inc.: Wallingford, CT, 2016.

https://doi.org/10.1021/acs.jpclett.4c02979
J. Phys. Chem. Lett. 2024, 15, 12494−12500